Acetaminophen Overdose Reveals Protease-Activated Receptor 4 as a Low-Expressing but Potent Receptor on the Hepatic Endothelium

Rahul Rajala[1,2,3], Audrey C.A. Cleuren[1,2], Courtney T. Griffin[1,2,*]

[1]Cardiovascular Biology Research Program, Oklahoma Medical Research Foundation, Oklahoma City, OK

[2]Department of Cell Biology, University of Oklahoma Health Sciences Center, Oklahoma City, OK

[3]Harold Hamm Diabetes Center, Oklahoma City, OK

Short Title: APAP Overdose Reveals Functional PAR4 on Liver ECs

***Corresponding Author:** Courtney T. Griffin; 825 NE 13th Street; Oklahoma City, OK, 73104; Phone: 405-271-7073; Fax: 405-271-3137; e-mail: courtney-griffin@omrf.org

Keywords: PAR1, PAR4, TRAP, Vasculature, APAP

ABSTRACT

Background & Aims: Hepatic endothelial cell (EC) dysfunction and centrilobular hepatocyte necrosis occur with acetaminophen (APAP) overdose. The protease thrombin, which is acutely generated during APAP overdose, can signal through protease-activated receptors 1 and 4 (PAR1/PAR4). PAR1 is a high-affinity thrombin receptor that is known to signal on ECs, whereas PAR4 is a low-affinity thrombin receptor, and evidence for its expression and function on ECs is mixed. This study aims to exploit the high levels of thrombin generated during APAP overdose to determine (1) if hepatic endothelial PAR4 is a functional receptor, and (2) endothelial-specific functions for PAR1 and PAR4 in a high thrombin setting.

Methods: We generated mice with conditional deletion(s) of *Par1/Par4* in ECs and overdosed them with APAP. Hepatic vascular permeability, erythrocyte congestion/bleeding, and liver function were assessed following overdose. Additionally, we investigated the expression levels of endothelial PARs and how they influence transcription in APAP-overdosed liver ECs using endothelial Translating Ribosome Affinity Purification followed by next-generation sequencing (TRAPseq).

Results: We found that mice deficient in high-expressing endothelial *Par1* or low-expressing *Par4* had equivalent reductions in APAP-induced hepatic vascular instability but no effect on hepatocyte necrosis. Additionally, mice with loss of endothelial *Par1* and *Par4* had reduced permeability at an earlier time point after APAP overdose when compared to mice singly deficient in either receptor in ECs. We also found that endothelial PAR1—but not PAR4—can regulate transcription in hepatic ECs.

Conclusions: Low-expressing PAR4 can react similarly to high-expressing PAR1 in APAP-overdosed hepatic ECs, demonstrating that PAR4 is a potent thrombin receptor. Additionally, these receptors are functionally redundant but act divergently in their expression and ability to influence transcription in hepatic ECs.

NON-STANDARD ABBREVIATIONS AND ACRONYMS

ALT, Alanine Aminotransferase; APAP, Acetaminophen; AST, Aspartate Aminotransferase; ECs, Endothelial Cells; GO, Gene Ontology; GPCR, G Protein-Coupled Receptor; HUVECs, Human Umbilical Vein Endothelial Cells; IPA, Ingenuity Pathway Analysis; NAPQI, N-acetyl-p-benzoquinone imine; PAR1, Protease-Activated Receptor 1; PAR4, Protease-Activated Receptor 4; RBCs, Red Blood Cells; TPM, Transcripts Per Million; TRAP, Translating Ribosome Affinity Purification

NOMENCLATURE

F2r and *F2rl3* are the gene names for PAR1 and PAR4, respectively. For simplicity, we hereafter refer to these genes as *Par1* and *Par4.*

INTRODUCTION

The vascular endothelium, which forms the inner lining of blood vessels, is a sprawling cell layer covering a total surface area of 270-720 square meters[1]. Endothelial cells (ECs) participate in the regulation of tissue function and structure, the trafficking of hormones and nutrients[2], the control of inflammation[3], and the regulation of vascular permeability [4]. With these critical and diverse roles, it is not surprising that endothelial dysfunction amplifies various pathological insults in specific organs[4-6].

Protease-activated receptors (PARs) are a family of G protein-coupled receptors (GPCRs) with four members (PAR1-4). PAR1 and PAR4 are thrombin receptors that have been linked to many physiological processes and that are associated with pathologies like diabetes, Alzheimer's disease, and cancer when dysregulated[7]. These receptors have different affinities for thrombin (PAR1: 50 pM and PAR4: 5000 pM)[8], as well as distinct mechanisms for signaling[9-11] and desensitization[7,12]. PARs can act synergistically or redundantly and can directly dimerize to enact a biased signaling response[13]. Both PAR1 and PAR4 are expressed on ECs; however, endothelial PAR4 is expressed at low levels, so there is a paucity of data on its function[14]. For example, since the receptor was reported to be present and functional on mouse ECs in the early 2000s[15,16], only about 90 subsequent papers about endothelial PAR4 have been published. Among those papers, approximately one in six has reported that PAR4 is non-functional on ECs. Some of this controversy about the functionality of endothelial PAR4 may be explained by its low or undetectable expression on cultured ECs, including primary human umbilical vein ECs (HUVECs) that are broadly used for EC research. The lack of suitable *in vitro* tools to study endothelial PAR4 has led to the prevailing theory that PAR4 is an inconsequential thrombin receptor on ECs. However, knowing that cultured ECs can undergo phenotypic drift that results in divergent gene expression patterns from *in vivo* ECs[17,18], we recognized a need to assess endothelial PAR4 function *in vivo* with cell-specific gene deletions in a setting of high thrombin generation.

In this study, we chose acetaminophen (APAP) overdose as a model for exploring endothelial PAR4 and PAR1 functionality. APAP overdose is the leading cause of acute liver injury in the United States[19]. The pathology of APAP is characterized by centrilobular hepatocyte necrosis and congestion of sinusoidal

blood vessels[19]. Importantly for this study, thrombin levels are significantly increased during APAP overdose, making this an ideal model to study the function of endothelial thrombin receptors, and both PAR1 and PAR4 have been shown to contribute to APAP pathology in mice[20,21]. However, previous studies have used global knockout (KO) mice to study PAR1 and PAR4 in the context of APAP overdose, which makes it difficult to dissect cell-specific roles for these receptors in the hepatic niche. For example, *Par4*$^{-/-}$ mice have less liver damage than wildtype mice at 6 and 24 hours after APAP overdose, as indicated by reduced hepatocyte necrosis and plasma alanine aminotransferase (ALT) activity[21]. However, when bone marrow from *Par4*$^{-/-}$ deficient mice was transplanted into irradiated wildtype mice, the beneficial reduction in hepatocyte necrosis and ALT activity was lost[21]. The authors of this study speculated that the cell-specific loss of PAR4 on ECs—rather than on platelets, where it is robustly expressed—was responsible for the reduced hepatocyte necrosis seen in *Par4*$^{-/-}$ mice after APAP overdose[15]. Similarly, *Par1*$^{-/-}$ mice have reduced plasma ALT levels compared to wildtype mice at 6 hr following APAP overdose[20], but it is not clear if this can be attributed to loss of PAR1 on hepatocytes or on sinusoidal ECs, where the receptor is most robustly expressed[22].

To determine the impact of endothelial PAR4 and PAR1 on liver vasculature and hepatocytes after APAP overdose, our current study utilized newly generated *Par4*- and *Par1*- floxed alleles to achieve conditional deletion of the receptors in ECs of adult mice. Our findings highlight: (1) the presence of functional endothelial PAR4 *in vivo,* (2) independent and interdependent roles for PAR1 and PAR4 on liver ECs, and (3) a clarification of the relationship between endothelial PAR-mediated vascular damage and hepatocyte necrosis following APAP overdose.

MATERIALS AND METHODS

The data that support the findings of this study are available from the corresponding author upon request. Materials and methods can be found in Supplemental Materials, and detailed information about the resources used in this study is listed in the Major Resources Table.

RESULTS

Deletion of endothelial *Par1* and/or *Par4* reduces APAP-induced hepatic vascular permeability with distinct kinetics

Endothelial PARs are often studied in the context of vascular permeability, so we initially sought to determine if loss of *Par4* and/or *Par1* on ECs reduced APAP-induced hepatic vascular permeability in mice. We first generated mice with floxed alleles of each receptor. LoxP sites were inserted flanking the first exon of *Par1* and *Par4* (Supplementary Fig. S1A-C), and mice carrying the floxed alleles were identified by PCR genotyping (Supplementary Fig. S1D). In addition to maintaining each floxed line separately, we also generated mice carrying both floxed alleles. This decision was based on the fact that PAR1 and PAR4 can directly interact with each other and can both be activated by thrombin, although PAR1 has a higher affinity for thrombin through its hirudin-like domain (Supplementary Fig. S2)[13]. We next crossed our floxed alleles to the tamoxifen-inducible *Cdh5(PAC)-Cre*^{ERT2} line[23], which is expressed exclusively in ECs when induced in adult mice[24]. The use of an inducible Cre was warranted because the endothelial-specific loss of *Par1* during embryonic development is partially lethal[25], which would hinder the generation of experimental mice needed for our studies. This approach produced inducible single- and double-EC knockout alleles for *Par1* and *Par4* (hereafter, *Par1*^{iECko}, *Par4*^{iECko}, and *Par1/4*^{iECko}).

Experimental mice were administered 5 doses of tamoxifen (total of 10 mg) at 5-6 weeks of age for Cre induction. Cre-negative littermate control mice received the same regime. After the final tamoxifen dose, mice were allowed to acclimate for 4 weeks to achieve complete deletion of *Par4* and/or *Par1* and to avoid confounding results from tamoxifen-induced liver dysfunction[26]. Experimental mice were fasted for 16 hr to deplete hepatic glutathione stores and were subsequently administered 300 mg/kg APAP, or a saline vehicle control (Figure 1A). Following the administration of APAP or saline, hepatic vascular permeability

was assessed at 6 and 24 hr by assessing leakage of intravascular Evans blue dye (Figure 1B). Basal hepatic permeability at all time points was determined to be 55 ng/mg of Evans blue (shown as a reference line in Figure 1C), with no significant difference between wildtype and *Par*^{iECko} mice.

Administration of APAP resulted in a significant increase in liver permeability in control mice at 6 hr (~9.1-fold) and at 24 hr (~10.2-fold) compared to saline. This APAP-induced vascular permeability was significantly reduced in *Par1/4*^{iECko} mice at both 6 hr (~46.2%) and 24 hr (~41.3%) compared to Cre-negative littermate controls. By contrast, vascular permeability was not reduced in *Par1*^{iECko} mice at 6 hr after APAP overdose but was reduced after 24 hr (~43.1%). Similarly, vascular permeability was not reduced in *Par4*^{iECko} mice at 6 hr after APAP overdose, but it was reduced at 24 hr (~40.0%), comparable to levels seen in *Par1/4*^{iECko} and *Par1*^{iECko} mice. These data indicate that loss of endothelial PAR1 and/or PAR4 is sufficient to reduce APAP-induced permeability in the liver, with dual loss of the receptors reducing permeability at 6 hours, and single loss of PAR1 or PAR4 reducing permeability only at 24 hours. These data also demonstrate that PAR4 is a functional receptor on hepatic ECs and that it mediates vascular permeability comparably to PAR1 after APAP overdose.

Deletion of endothelial *Par1* and/or *Par4* also reduces APAP-induced sinusoidal congestion in mice

Since our data indicated that loss of endothelial PARs reduced APAP-induced vascular permeability, we sought to determine if additional measures of vascular function were rescued in *Par*^{iECko} mice. APAP overdose causes congestion of hepatic sinusoids and accumulation of red blood cells (RBCs) around the central veins, overlapping with regions of zone 3 hepatocyte necrosis[27]. This phenotype was observed in our control mice, as evidenced by H&E staining at 24 hr after APAP overdose (Fig. 2). However, we observed reduced RBC congestion in APAP-treated *Par1/4*^{iECko} mice compared to littermate controls (~39.5%; Fig. 2A). We likewise saw reduced congestion in *Par1*^{iECko} mice (~34.6%; Fig. 2B) and *Par4*^{iECko} mice (~35.3%; Fig. 2C) compared to littermate controls. Moreover, *Par1/4*^{iECko} did not have significantly more reduction in congestion compared to mice singly deficient in *Par1* or *Par4* (Supplementary Fig. S3A), which suggests that loss of one or both receptors is equally effective at reducing RBC congestion after APAP overdose.

PAR4 has been best characterized in platelets, where it is highly expressed[22], and it is typically observed to have low expression levels in ECs[14]. To ensure our rescued RBC congestion phenotype was not influenced by ectopic deletion of *Par4* in platelets, we generated platelet-specific *Par4* knockouts (*Par4*^{PLTko}) by crossing *Par4*-flox mice to a *Pf4-Cre* line. Unlike *Par4*^{iECko} mice, *Par4*^{PLTko} mice did not show reduced RBC congestion compared to littermate controls after APAP overdose ($p<0.9954$; Fig 2D). Therefore, PAR4 on ECs—rather than on platelets—contributes to sinusoidal congestion after APAP overdose, further confirming that PAR4 is a functional receptor on the hepatic endothelium.

Deletion of endothelial *Par1* and/or *Par4* does not reduce APAP-induced hepatic injury

To determine if the reduced APAP-induced vascular instability seen in *Par*^{iECko} mice correlated with reduced hepatic injury, we collected livers and serum from *Par*^{iECko} and littermate controls after APAP overdose. Histological analyses revealed that control mice displayed severe necrosis of zone 3 hepatocytes surrounding hepatic central veins at 6 hr after APAP overdose, and we saw comparable necrosis in livers from *Par1/4*^{iECko}, *Par1*^{iECko}, *Par4*^{iECko}, and *Par4*^{PLTko} mice (Fig. 3 and Supplementary Fig. S3B). Since vascular permeability and sinusoidal congestion were most robustly rescued in APAP-treated *Par1/4*^{iECko} mice, we further analyzed hepatic injury in these mutants by measuring serum ALT/AST levels at 6 hr and 24 hr after APAP overdose. Serum ALT (Fig. 3E) and AST (Fig. 3F) levels were similar between *Par1/4*^{iECko} and littermate controls, indicating that loss of endothelial PARs and reductions in vascular permeability and sinusoidal congestion do not alleviate APAP-induced hepatic injury.

Translating Ribosome Affinity Purification (TRAP) reveals distinct endothelial responses to APAP overdose

Since endothelial PAR1 and PAR4 contributed to vascular dysfunction following APAP overdose, and GPCR signaling can modulate transcription[28], we next wanted to assess how PAR1 and PAR4 impacted transcripts in liver ECs using translating ribosome affinity purification followed by next-generation sequencing (TRAPseq; Fig. 4A). We used RiboTag mice for this technique, in which Cre-mediated recombination labels the ribosomal protein RPL22 with an HA tag to facilitate cell-specific isolation of

actively translating mRNA. We crossed the RiboTag cassette onto our *Par1*^{iECko} and *Par4*^{iECko} mice, and we used RiboTag-*Par1*^{iEChet} and RiboTag-*Par4*^{iEChet} mice as littermate controls since the RiboTag cassette only activates in response to a Cre recombinase. We then collected livers from RiboTag-*Par1*^{iEChet}, RiboTag-*Par4*^{iEChet}, RiboTag-*Par1*^{iECko}, and RiboTag-*Par4*^{iECko} mice (3 animals from each genotype) at 6 hr following saline or APAP treatment. Note that the 6 hr time point was chosen for all analyses because it preceded the reduced vascular permeability and sinusoidal congestion seen in *Par1*^{iECko} and *Par4*^{iECko} mice and might reveal endothelial transcriptional changes associated with those phenotypes. Furthermore, thrombin levels are significantly elevated by this time after APAP overdose[20,21]. Each liver sample was then homogenized and immunoprecipitated to isolate endothelium-specific mRNA from the liver mRNA, thereby allowing us to identify changes in both total liver transcripts and endothelial-specific transcripts after APAP overdose by RNAseq.

Our RNAseq data were then run through a custom analysis pipeline (Supplemental Fig. S4), and the results were subjected to principal component analysis, which showed distinct separation of groups by treatment and fraction (Fig. 4B). In control mice, APAP overdose dramatically affected the transcriptional profiles of the liver when we compared differential gene expression; out of 13,189 genes assayed, 6,169 (~46.7%) had significant expression changes ($P_{adj}<0.05$) after APAP treatment (Fig. 4C). We next performed Qiagen Ingenuity Pathway Analysis (IPA) on these RNAseq results. Network analysis revealed predicted APAP-induced activation of TNF, IL-1β, IL-6, and EGF (Supplemental Fig. S5A). Furthermore, IPA pathway analysis predicted the upregulation of oxidative phosphorylation, uncoupling proteins, and eukaryotic translation, elongation, and termination in the liver (Supplemental Fig. S5B). These are reasonable predictions since APAP overdose causes oxidative injury and inflammation[19].

To assess the efficacy of the TRAP enrichment, we compared the transcriptional profiles from endothelium-enriched fractions versus total liver in our saline-treated control animals (Supplemental Fig. S6A). To validate that the TRAP-enriched transcripts were endothelial, we screened the top 500 enriched genes with Gene Ontology (GO; https://geneontology.org/)[29]. The GO terms included pathways commonly associated with ECs, such as "sprouting angiogenesis," "positive regulation of endothelial cell

proliferation," and "VEGFR signaling pathway" (Supplemental Fig. S6B). We next assessed how APAP overdose affected the endothelial gene expression profiles in control mice. We first removed all TRAP-depleted genes (i.e., genes enriched in non-ECs) from our endothelial dataset. Out of 12,248 genes assayed in the endothelium, we observed significant shifts in 1,858 genes after APAP overdose (~15.2%; Fig. 4D). IPA network analysis revealed similar driving factors to those we saw in the liver after APAP overdose (i.e., TNF, IL-1β, and EGF) (Supplemental Fig. S5C). However, pathway analysis indicated that endothelial responses predominantly had themes of altered signaling, such as signaling through interleukins, estrogen receptor, phosphatase and tensin homolog (PTEN), and actin-binding rho activating protein (ABRA) (Supplemental Fig. S5D). Comparing alterations in IPA-identified pathways between the liver and endothelium after APAP overdose, we found unique pathways for each fraction (Fig. 4E and Supplemental File 1).

Endothelial TRAP quantification of *Par1* and *Par4*

Due to the limited expression of PAR4 on only a few cell types[22], including its low expression in many ECs[30], single-cell RNAseq (scRNAseq) is usually unable to quantify *Par4* expression since this technique favors the identification of high-expressing transcripts in individual cells[31]. Endothelial TRAP, however, facilitates the aggregation of transcripts from all ECs in an organ, which allowed us to measure actively translating *Par1* and *Par4* transcripts in hepatic ECs. Our TRAP data indicated that both *Par1* and *Par4* are endothelial-enriched genes (Fig. 5). Moreover, using a SALMON RNAseq pipeline, we were able to compare the normalized expression of *Par1* and *Par4* in hepatic ECs; *Par1* was expressed at 85.8 transcripts per million (TPM), and *Par4* was expressed at 0.56 TPM. Therefore, there are 153 *Par1* transcripts for every *Par4* transcript in the hepatic endothelium, whereas there are 43 *Par1* transcripts for every *Par4* transcript in the total liver (Supplemental File 2).

The 153:1 ratio of *Par1* to *Par4* transcripts on hepatic ECs is particularly interesting since our genetic deletion data demonstrate that PAR1 and PAR4 mediate the same vascular responses to APAP overdose (Fig 1C and Supplemental Fig. S3). This indicates that PAR4 is a low-expressing but potent receptor on hepatic ECs. PAR4 undergoes limited desensitization following activation and therefore can strongly

amplify signaling through second messengers[12,32,33], which may account for its robust response in the setting of APAP overdose. Additionally, this disproportionate *Par1:Par4* expression ratio suggests that PAR1-PAR4 heterodimers are unlikely to contribute to a significant portion of the PAR dimer pool on hepatic ECs *in vivo*, especially when compared to PAR1-PAR1 homodimers. Finally, we did not find *Par2* or *Par3* expression in the hepatic endothelium (Supplemental File 2), which makes liver ECs ideal for studying PAR1/PAR4-specific signaling effects in the absence of the other PARs.

Characterizing how endothelial PARs interact and respond to APAP using TRAPseq

We next sought to understand how the loss of endothelial PAR1 or PAR4 affected transcriptional profiles in the liver and endothelium. We first validated *Par1* and *Par4* deletion from ECs in our RiboTag-*Par1*^{iECko} and RiboTag-*Par4*^{iECko} mice, respectively. We found an appropriate reduction in *Par1* and *Par4* transcripts in EC fractions from RiboTag-labeled endothelial heterozygous and knockout *Par1* and *Par4* mice, respectively (Fig. 5A, B). *Par1* expression was reduced in the endothelium by ~99.9% when comparing RiboTag-labeled *Par1*^{iECko} and *Par1*^{ECwt} mice, while endothelial *Par4* expression was reduced by ~94% when comparing RiboTag-labeled *Par4*^{iECko} and *Par4*^{ECwt} mice. We also found that deletion of endothelial *Par4* did not influence *Par1* expression under basal (i.e., saline-treated) conditions, based on the liver and endothelial fractions from RiboTag-labeled *Par4*^{iEChet} and *Par4*^{iECko} mice (Fig. 5C). Likewise, deletion of endothelial *Par1* did not influence *Par4* expression under basal conditions (Fig. 5D).

Following APAP overdose in RiboTag-*Par1*^{iEChet} (control) mice, we found significantly reduced expression of endothelial *Par4* compared to saline-treated control mice (66.0%, $p<0.0078$; Fig. 5C). However, this reduction in endothelial *Par4* was completely abolished in APAP- versus saline-treated *Par1*^{iECko} mice (Fig. 5C), suggesting that PAR1 regulates *Par4* expression after APAP overdose. Similarly, we found reduced expression of endothelial *Par1* (~61.1%, $p<0.0041$) in APAP- versus saline-treated RiboTag-*Par4*^{iEChet} (control) mice (Fig. 5D). This reduction was diminished in *Par4*^{iECko} mice (~28.1%, $p<0.1469$) (Fig. 5D), suggesting that PAR4 may likewise regulate *Par1* expression after APAP overdose.

Endothelial PAR1 and PAR4 differentially regulate hepatic and endothelial gene expression changes to APAP overdose

We next assessed how endothelial *Par1* or *Par4* deletion affects the transcriptional profile of the liver after APAP overdose. First, we compared the liver gene expression profiles between RiboTag-labeled *Par1*^{iEChet} mice and *Par1*^{iECko} mice at 6 hr after APAP treatment. TRAPseq revealed 345 differentially expressed genes in the *Par1*^{iECko} mice (Supplemental Fig. S7A). Subsequent IPA network and pathway analyses indicated a reduction in genes involved in eukaryotic initiation factor 2 (EIF2) signaling (Supplemental Fig. S7B and C). Notably, when all the pathways that were altered by APAP overdose in the livers of RiboTag-*Par1*^{iEChet} mice were considered, only a small fraction (~7%) were rescued in RiboTag-*Par1*^{iECko} mice (Supplemental Fig. S7D). We also compared the liver gene expression profiles from RiboTag-labeled *Par4*^{iEChet} mice and *Par4*^{iECko} mice after APAP overdose, but we did not find any significant differences between these control and mutant samples (Supplemental Figure S8).

Finally, we sought to identify how endothelial deficiency of PAR1 and PAR4 affected hepatic endothelial gene expression after APAP overdose. We first compared the endothelium of RiboTag-labeled *Par1*^{iEChet} mice and *Par1*^{iECko} mice after APAP overdose. TRAPseq revealed 49 differentially expressed genes (Fig. 6A), and IPA pathway analyses indicated a reduction in genes involved in the pathways of "Rho GTPase cycle," and "phagosome formation" (Fig. 6C). IPA network analysis of overlapping pathways from these samples suggested the "Rho GTPase cycle" to be a central node (Supplemental Fig. S9). Further analysis revealed an increase in the expression of several genes involved in processes related to cytoskeletal rearrangement, phagocytosis, and vascular permeability in APAP-treated control endothelium, and these genes were rescued in APAP-treated *Par1*^{iECko} endothelium (Fig 6D). Alterations in genes involved in the Rho GTPase cycle and cytoskeletal rearrangement are notable since PAR1 is known to regulate these processes post-translationally[34,35]. These new TRAP data indicate that PAR1 may also impact these cellular processes at the level of transcription. We also found upregulated expression of AP-2 complex subunit beta (*Ap2b1*) in APAP-treated control endothelium and rescue of this gene in APAP-treated *Par1*^{iECko} endothelium (Fig 6D). Since AP-2 is involved in the endocytosis and trafficking of PAR1 and PAR4[36,37], *Ap2b1* transcriptional upregulation following PAR1 activation may facilitate increased trafficking of PARs

to maintain EC thrombin responsiveness after APAP overdose. Note that downregulated *Dll4* served as a positive control for our dataset since it has been reported to drop in expression in ECs after APAP overdose (Fig 6D)[38]. Finally, when we compared the endothelium of RiboTag-labeled *Par4*^{iEChet} mice and *Par4*^{iECko} mice after APAP overdose, we did not find significant differences between the samples (Fig. 6B). Therefore, PAR1 mediates transcriptional changes in ECs with APAP overdose, but PAR4 does not.

DISCUSSION

After two decades of controversy, our study demonstrates the presence of functional PAR4 on hepatic ECs *in vivo*. Our TRAP data reveal that both *Par1* and *Par4* are enriched in ECs of the murine liver, although endothelial *Par4* transcripts are expressed at low levels compared to *Par1* (1:153; Supplemental File 2). Importantly, *Par4*^{iECko} mice phenocopy both the reduced sinusoidal congestion and vascular permeability phenotypes seen in *Par1*^{iECko} mice after APAP overdose, indicating that endothelial PAR4 is a potent receptor despite its low expression.

Our study also shows that endothelial PAR1 and PAR4 contribute to hepatic vascular permeability and sinusoidal congestion after APAP overdose, since these phenotypes were attenuated in *Par*^{iECko} mice. Interestingly, dual loss of endothelial *Par1/4* reduced hepatic permeability at both early (6 hr) and late (24 hr) time points after APAP overdose, while loss of either individual receptor only reduced permeability at 24 hr, suggesting that endothelial PAR1 and PAR4 act redundantly to promote vascular instability 6 hours after APAP overdose.

Another important insight from this study is that vascular permeability does not have a significant impact on the hepatocyte necrosis seen at 6 hr after APAP overdose. Centrilobular hepatocyte necrosis is driven by elevated production of N-acetyl-p-benzoquinone imine (NAPQI), a toxic intermediate of APAP metabolism that is generated by the enzyme CYP-4502E1, which is primarily expressed in centrilobular hepatocytes[39,40]. Because of the hepatocyte-specific expression of CYP-4502E1, it is reasonable that NAPQI production and subsequent hepatocyte necrosis would not be altered in endothelial *Par*-deficient mice after APAP overdose. We believe previous studies that used global KO strategies to deplete PARs likely saw reduced hepatocyte necrosis after APAP overdose due to the loss of low-expressing PARs on hepatocytes[20,21]. Future studies can use hepatocyte-specific deletion of PARs to test this hypothesis.

Concordant changes in both hepatic vascular permeability and sinusoidal congestion after APAP overdose are understandable since both are measures of vascular stability. Previous studies have shown that sinusoidal ECs display gaps after APAP overdose through which RBCs can extravasate[27,41-43]. We observed

comparably reduced congestion/bleeding in both single- and double-*Par1/4*^{iECko} mice at 24 hr after APAP overdose. PAR1 can regulate endothelial shape change and vascular permeability either through $G\alpha_q$/phospholipase C-β /calmodulin/myosin light chain kinase signaling or through cytoskeleton rearrangements mediated by $G\alpha_{12/13}$/Rho-GTPase signaling[44]. PAR4 also regulates actin rearrangements in ECs[45]. Deletion of endothelial PARs likely makes liver ECs functionally insensitive to elevated thrombin levels, which are associated with APAP overdose[20,21]. As a result, reduced thrombin-induced EC shape changes may account for increased vascular stability in *Par*^{iECko} mice.

Although our study addresses the existence and function of PAR4 on liver ECs, we recognize that some of the initial controversy about endothelial PAR4 arose because of conflicting data generated from ECs in other organs. For example, Kataoka et al demonstrated that PAR4 is functional in murine pulmonary ECs in 2003[15], but others have since failed to reproduce those results[4]. This made us curious about *Par4* expression levels in ECs from lungs and other organs. Therefore, we surveyed *Par1* and *Par4* expression in murine ECs from multiple organs by looking at datasets generated by Kalucka et al[30] and Cleuren et al[17]. We found that *Par1* was expressed in ECs of most organs that were analyzed. *Par4*, on the other hand, had endothelial expression limited to the kidney, heart, liver, colon, and spleen (Supplemental Figure S10). This suggests that endothelial PAR4 may function most prominently in these organs *in vivo* and is consistent with the roles we identified for PAR4 in hepatic ECs in this study.

We also surveyed an RNAseq dataset by Buglak et al[46] and found that cultured HUVECs exposed to shear stress undergo significant upregulation of *PAR4* (~13.3-fold), although similar upregulation is not seen for *PAR1* (Supplemental Figure S11). Concordantly, scRNAseq analysis of human liver[47] indicates that endothelial *PAR4* expression is most prominent around the portal vein, where flow rates are highest[48] (Supplemental Figure S12D). Likewise, increased PAR4 levels have been detected in higher caliber pulmonary vessels, which have higher flow rates[49]. Since PAR4 is activated by circulating proteases, and high blood flow rates would decrease the local ligand residency time and availability for a given receptor, these expression data suggest that high protease concentrations would be required for PAR4 activation under high flow conditions.

Altogether, PAR4 appears to be a selectively expressed and low-affinity thrombin receptor on ECs in contrast to PAR1. However, our study indicates that PAR4 is a potent receptor that is capable of mediating similar responses to PAR1 in hepatic ECs. We hypothesize that the primary role of endothelial PAR4 is to maintain thrombin responsiveness in scenarios where the enzyme is present at high concentrations and has saturated endothelial PAR1 signaling. In addition, because PAR4 has limited desensitization mechanisms and can strongly amplify second messengers[12,32,33], its low expression is not indicative of a failure to function, but rather, it serves to limit the signaling of the receptor except in response to high thrombin activity, such as occurs with APAP overdose.

Notably, our TRAPseq data demonstrate that PAR1 and PAR4 show distinct differences in influencing EC transcriptional reprogramming after APAP overdose. Two interesting genes were *Par1* and *Par4* themselves, especially since the receptors facilitated downregulation of each other after APAP overdose. We attribute these changes to be due to receptor trans-downregulation, in which the activation of one PAR downregulates the other. We identified 49 other targets that were differentially expressed in *Par1*-deficient ECs, but no other genes were affected by *Par4* deletion. Given that both $Par1^{iECko}$ and $Par4^{iECko}$ mice display a reduction in permeability and sinusoidal congestion after APAP overdose, the gene expression changes in $Par1^{iECko}$ mice are unlikely to result from secondary effects of stabilizing the hepatic vasculature but rather from direct loss of PAR1 in hepatic ECs.

Several of the genes that we found differentially expressed in $Par1^{iECko}$ mice are linked to cellular permeability. These gene changes may not be functionally consequential in APAP overdose, since both $Par1^{iECko}$ and $Par4^{iECko}$ mice had reduced vascular permeability after APAP overdose even without comparable transcriptional changes, but they may be relevant in other models of thrombin-induced permeability or in organs lacking endothelial PAR4 (Supplemental Figure S10). Given that endothelial PAR4 is a potent signaling receptor and lacks desensitization mechanisms like PAR1, it might be best to limit PAR4 signaling effects to post-translational activities since unregulated transcription could be deleterious to long-term EC health and function. Altogether, our findings indicate that endothelial PAR1

and PAR4 are functionally redundant in regulating vascular stability but are distinct in their expression, signaling, and potency.

LIMITATIONS OF STUDY

TRAPseq represents a leap forward in our ability to quantify low-expressing genes like *Par4*. Although this technology allowed us to identify the ratio of actively translating *Par1:Par4* transcripts in hepatic ECs *in vivo*, one limitation we have is that we cannot claim that this ratio reflects the ratio of the receptors at the EC surface. Future studies using genetic mouse models to label endogenous proteins *in vivo*, such as FUNCAT[50], may be able to provide a better approximation of the true *in vivo* EC surface expression ratio of these receptors. Another limitation to this study is the lack of mechanistic insight into how PARs reduce endothelial permeability and sinusoidal congestion in the liver. Theoretically, we might have used cultured ECs to address this question, but this study highlights how static ECs are unsuitable for studying PAR4. Moreover, other labs have shown that PAR4 can mediate permeability by regulating cytoskeleton rearrangement and EC shape change through G protein-dependent and -independent signaling[45,51,52]. Therefore, we elected to focus instead on addressing the long-standing controversy on whether PAR4 is even present and functional in the vascular endothelium through our in vivo studies.

ACKNOWLEDGEMENTS

We thank Jun Xie, M.D., for assistance with mouse colony maintenance. We thank Christopher Bottoms, Ph.D., for his help with the OMRF cluster. Data processing and analysis were supported by the OMRF Center for Biomedical Data Sciences. Diagrams were created with BioRender.com.

SOURCES OF FUNDING

This work was supported by a grant to C.T.G. from the National Institutes of Health (R35HL144605) and predoctoral fellowships to R.R. from the American Heart Association (23PRE1014240) and OMRF.

AUTHOR CONTRIBUTIONS

R.R. designed and conducted all experiments and analyses, including the writing of all the informatics programs used in the manuscript. A.C.A.C. prepared immunoprecipitated RNA into libraries for sequencing. R.R. wrote the manuscript. C.T.G. oversaw the project and edited the manuscript. All authors provided critical feedback that helped shape the research, analysis, and manuscript.

DATA AVAILABILITY

The data reported in this paper have been deposited in the Gene Expression Omnibus (accession no. GSE266395).

SUPPLEMENTAL MATERIALS

Supplemental Figures S1-S12

Methods and Materials

List of online supplemental files: SF1-SF5

Supplemental Tables: ST1-ST3

Major Resource Table: ST4

Supplemental References

DISCLOSURES

The authors have no conflicts of interest to disclose.

REFERENCES

1. Rajala R. How big is the endothelium? Comment on "Spatial and temporal dynamics of the endothelium". *J Thromb Haemost*. 2021;19:2634-2635. doi: 10.1111/jth.15469
2. Lee WL, Klip A. Endothelial Transcytosis of Insulin: Does It Contribute to Insulin Resistance? *Physiology (Bethesda)*. 2016;31:336-345. doi: 10.1152/physiol.00010.2016
3. Pober JS, Sessa WC. Evolving functions of endothelial cells in inflammation. *Nat Rev Immunol*. 2007;7:803-815. doi: 10.1038/nri2171
4. Mehta D, Malik AB. Signaling mechanisms regulating endothelial permeability. *Physiol Rev*. 2006;86:279-367. doi: 10.1152/physrev.00012.2005
5. Park KH, Park WJ. Endothelial Dysfunction: Clinical Implications in Cardiovascular Disease and Therapeutic Approaches. *J Korean Med Sci*. 2015;30:1213-1225. doi: 10.3346/jkms.2015.30.9.1213
6. Krüger-Genge A, Blocki A, Franke R-P, Jung F. Vascular Endothelial Cell Biology: An Update. *International journal of molecular sciences*. 2019;20:4411. doi: 10.3390/ijms20184411
7. Adams MN, Ramachandran R, Yau M-K, Suen JY, Fairlie DP, Hollenberg MD, Hooper JD. Structure, function and pathophysiology of protease activated receptors. *Pharmacology & therapeutics*. 2011;130:248-282.
8. Steinberg SF. The cardiovascular actions of protease-activated receptors. *Molecular pharmacology*. 2005;67:2-11.
9. Momota F, Hirano K, Hirano M, Nishimura J, Kanaide H. Involvement of Gi/o in the PAR-4-induced NO production in endothelial cells. *Biochem Biophys Res Commun*. 2006;342:365-371. doi: 10.1016/j.bbrc.2006.01.165
10. Hirano K, Nomoto N, Hirano M, Momota F, Hanada A, Kanaide H. Distinct Ca2+ requirement for NO production between proteinase-activated receptor 1 and 4 (PAR1 and PAR4) in vascular endothelial cells. *J Pharmacol Exp Ther*. 2007;322:668-677. doi: 10.1124/jpet.107.121038
11. Dangelmaier C, Kunapuli SP. Protease-activated receptor 4 causes Akt phosphorylation independently of PI3 kinase pathways. *Platelets*. 2020:1-6. doi: 10.1080/09537104.2020.1802415
12. Shapiro MJ, Weiss EJ, Faruqi TR, Coughlin SR. Protease-activated receptors 1 and 4 are shut off with distinct kinetics after activation by thrombin. *J Biol Chem*. 2000;275:25216-25221. doi: 10.1074/jbc.M004589200
13. Lin H, Liu AP, Smith TH, Trejo J. Cofactoring and dimerization of proteinase-activated receptors. *Pharmacol Rev*. 2013;65:1198-1213. doi: 10.1124/pr.111.004747
14. Fender AC, Rauch BH, Geisler T, Schror K. Protease-Activated Receptor PAR-4: An Inducible Switch between Thrombosis and Vascular Inflammation? *Thromb Haemost*. 2017;117:2013-2025. doi: 10.1160/th17-03-0219
15. Kataoka H, Hamilton JR, McKemy DD, Camerer E, Zheng YW, Cheng A, Griffin C, Coughlin SR. Protease-activated receptors 1 and 4 mediate thrombin signaling in endothelial cells. *Blood*. 2003;102:3224-3231. doi: 10.1182/blood-2003-04-1130
16. Camerer E, Kataoka H, Kahn M, Lease K, Coughlin SR. Genetic evidence that protease-activated receptors mediate factor Xa signaling in endothelial cells. *Journal of Biological Chemistry*. 2002;277:16081-16087.
17. Cleuren ACA, van der Ent MA, Jiang H, Hunker KL, Yee A, Siemieniak DR, Molema G, Aird WC, Ganesh SK, Ginsburg D. The in vivo endothelial cell translatome is highly heterogeneous across vascular beds. *Proc Natl Acad Sci U S A*. 2019;116:23618-23624. doi: 10.1073/pnas.1912409116
18. Amatschek S, Kriehuber E, Bauer W, Reininger B, Meraner P, Wolpl A, Schweifer N, Haslinger C, Stingl G, Maurer D. Blood and lymphatic endothelial cell-specific differentiation programs are stringently controlled by the tissue environment. *Blood*. 2007;109:4777-4785. doi: 10.1182/blood-2006-10-053280
19. Jaeschke H, Xie Y, McGill MR. Acetaminophen-induced Liver Injury: from Animal Models to Humans. *J Clin Transl Hepatol*. 2014;2:153-161. doi: 10.14218/jcth.2014.00014
20. Ganey PE, Luyendyk JP, Newport SW, Eagle TM, Maddox JF, Mackman N, Roth RA. Role of the coagulation system in acetaminophen-induced hepatotoxicity in mice. *Hepatology*. 2007;46:1177-1186. doi: 10.1002/hep.21779
21. Miyakawa K, Joshi N, Sullivan BP, Albee R, Brandenberger C, Jaeschke H, McGill MR, Scott MA, Ganey PE, Luyendyk JP, et al. Platelets and protease-activated receptor-4 contribute to

acetaminophen-induced liver injury in mice. *Blood*. 2015;126:1835-1843. doi: 10.1182/blood-2014-09-598656
22. Single-cell transcriptomics of 20 mouse organs creates a Tabula Muris. *Nature*. 2018;562:367-372. doi: 10.1038/s41586-018-0590-4
23. Wang Y, Nakayama M, Pitulescu ME, Schmidt TS, Bochenek ML, Sakakibara A, Adams S, Davy A, Deutsch U, Lüthi U, et al. Ephrin-B2 controls VEGF-induced angiogenesis and lymphangiogenesis. *Nature*. 2010;465:483-486. doi: 10.1038/nature09002
24. Kilani B, Gourdou-Latyszenok V, Guy A, Bats ML, Peghaire C, Parrens M, Renault MA, Duplàa C, Villeval JL, Rautou PE, et al. Comparison of endothelial promoter efficiency and specificity in mice reveals a subset of Pdgfb-positive hematopoietic cells. *J Thromb Haemost*. 2019;17:827-840. doi: 10.1111/jth.14417
25. Griffin CT, Srinivasan Y, Zheng YW, Huang W, Coughlin SR. A role for thrombin receptor signaling in endothelial cells during embryonic development. *Science*. 2001;293:1666-1670. doi: 10.1126/science.1061259
26. Gao FF, Lv JW, Wang Y, Fan R, Li Q, Zhang Z, Wei L. Tamoxifen induces hepatotoxicity and changes to hepatocyte morphology at the early stage of endocrinotherapy in mice. *Biomed Rep*. 2016;4:102-106. doi: 10.3892/br.2015.536
27. Gao S, Silasi-Mansat R, Behar AR, Lupu F, Griffin CT. Excessive Plasmin Compromises Hepatic Sinusoidal Vascular Integrity After Acetaminophen Overdose. *Hepatology*. 2018;68:1991-2003. doi: 10.1002/hep.30070
28. Klauer MJ, Willette BKA, Tsvetanova NG. Functional diversification of cell signaling by GPCR localization. *J Biol Chem*. 2024;300:105668. doi: 10.1016/j.jbc.2024.105668
29. Thomas PD, Ebert D, Muruganujan A, Mushayahama T, Albou LP, Mi H. PANTHER: Making genome-scale phylogenetics accessible to all. *Protein Sci*. 2022;31:8-22. doi: 10.1002/pro.4218
30. Kalucka J, de Rooij L, Goveia J, Rohlenova K, Dumas SJ, Meta E, Conchinha NV, Taverna F, Teuwen LA, Veys K, et al. Single-Cell Transcriptome Atlas of Murine Endothelial Cells. *Cell*. 2020;180:764-779.e720. doi: 10.1016/j.cell.2020.01.015
31. Rajala A, Rajala R, Gopinadhan Nair GK, Rajala RVS. Atlas of Phosphoinositide Signatures in the Retina Identifies Heterogeneity between Cell Types. *PNAS Nexus*. 2023. doi: 10.1093/pnasnexus/pgad063
32. Covic L, Gresser AL, Kuliopulos A. Biphasic kinetics of activation and signaling for PAR1 and PAR4 thrombin receptors in platelets. *Biochemistry*. 2000;39:5458-5467. doi: 10.1021/bi9927078
33. Ando S, Otani H, Yagi Y, Kawai K, Araki H, Nakamura T, Fukuhara S, Inagaki C. Protease-activated receptor 4-mediated Ca2+ signaling in mouse lung alveolar epithelial cells. *Life Sci*. 2007;81:794-802. doi: 10.1016/j.lfs.2007.06.026
34. Zhao L, Hu J, Zheng P, Mi B, Chen Z, Zhao X, Wu J, Wang Y. PAR1 regulates sepsis-induced vascular endothelial barrier dysfunction by mediating ERM phosphorylation via the RhoA/ROCK signaling pathway. *Int Immunopharmacol*. 2023;124:110992. doi: 10.1016/j.intimp.2023.110992
35. Lin Y, Wozniak JM, Grimsey NJ, Girada S, Patwardhan A, Molinar-Inglis O, Smith TH, Lapek JD, Gonzalez DJ, Trejo J. Phosphoproteomic analysis of protease-activated receptor-1 biased signaling reveals unique modulators of endothelial barrier function. *Proc Natl Acad Sci U S A*. 2020;117:5039-5048. doi: 10.1073/pnas.1917295117
36. Paing MM, Johnston CA, Siderovski DP, Trejo J. Clathrin adaptor AP2 regulates thrombin receptor constitutive internalization and endothelial cell resensitization. *Mol Cell Biol*. 2006;26:3231-3242. doi: 10.1128/mcb.26.8.3231-3242.2006
37. Smith TH, Coronel LJ, Li JG, Dores MR, Nieman MT, Trejo J. Protease-activated Receptor-4 Signaling and Trafficking Is Regulated by the Clathrin Adaptor Protein Complex-2 Independent of beta-Arrestins. *J Biol Chem*. 2016;291:18453-18464. doi: 10.1074/jbc.M116.729285
38. Ben-Moshe S, Veg T, Manco R, Dan S, Papinutti D, Lifshitz A, Kolodziejczyk AA, Bahar Halpern K, Elinav E, Itzkovitz S. The spatiotemporal program of zonal liver regeneration following acute injury. *Cell Stem Cell*. 2022;29:973-989.e910. doi: 10.1016/j.stem.2022.04.008
39. Yan M, Huo Y, Yin S, Hu H. Mechanisms of acetaminophen-induced liver injury and its implications for therapeutic interventions. *Redox Biol*. 2018;17:274-283. doi: 10.1016/j.redox.2018.04.019

40. Yoon E, Babar A, Choudhary M, Kutner M, Pyrsopoulos N. Acetaminophen-Induced Hepatotoxicity: a Comprehensive Update. *J Clin Transl Hepatol*. 2016;4:131-142. doi: 10.14218/jcth.2015.00052
41. Ito Y, Bethea NW, Abril ER, McCuskey RS. Early hepatic microvascular injury in response to acetaminophen toxicity. *Microcirculation*. 2003;10:391-400. doi: 10.1038/sj.mn.7800204
42. McCuskey RS. Sinusoidal endothelial cells as an early target for hepatic toxicants. *Clin Hemorheol Microcirc*. 2006;34:5-10.
43. McCuskey RS. The hepatic microvascular system in health and its response to toxicants. *Anat Rec (Hoboken)*. 2008;291:661-671. doi: 10.1002/ar.20663
44. Grimsey NJ, Trejo J. Integration of endothelial protease-activated receptor-1 inflammatory signaling by ubiquitin. *Curr Opin Hematol*. 2016;23:274-279. doi: 10.1097/moh.0000000000000232
45. Fujiwara M, Jin E, Ghazizadeh M, Kawanami O. Activation of PAR4 induces a distinct actin fiber formation via p38 MAPK in human lung endothelial cells. *J Histochem Cytochem*. 2005;53:1121-1129. doi: 10.1369/jhc.4A6592.2005
46. Buglak DB, Bougaran P, Kulikauskas MR, Liu Z, Monaghan-Benson E, Gold AL, Marvin AP, Burciu A, Tanke NT, Oatley M, et al. Nuclear SUN1 stabilizes endothelial cell junctions via microtubules to regulate blood vessel formation. *Elife*. 2023;12. doi: 10.7554/eLife.83652
47. MacParland SA, Liu JC, Ma XZ, Innes BT, Bartczak AM, Gage BK, Manuel J, Khuu N, Echeverri J, Linares I, et al. Single cell RNA sequencing of human liver reveals distinct intrahepatic macrophage populations. *Nat Commun*. 2018;9:4383. doi: 10.1038/s41467-018-06318-7
48. Wei W, Pu YS, Wang XK, Jiang A, Zhou R, Li Y, Zhang QJ, Wei YJ, Chen B, Li ZF. Wall shear stress in portal vein of cirrhotic patients with portal hypertension. *World J Gastroenterol*. 2017;23:3279-3286. doi: 10.3748/wjg.v23.i18.3279
49. Jesmin S, Gando S, Zaedi S, Sakuraya F. Differential expression, time course and distribution of four PARs in rats with endotoxin-induced acute lung injury. *Inflammation*. 2007;30:14-27. doi: 10.1007/s10753-006-9017-8
50. Alvarez-Castelao B, Schanzenbächer CT, Hanus C, Glock C, Tom Dieck S, Dörrbaum AR, Bartnik I, Nassim-Assir B, Ciirdaeva E, Mueller A, et al. Cell-type-specific metabolic labeling of nascent proteomes in vivo. *Nat Biotechnol*. 2017;35:1196-1201. doi: 10.1038/nbt.4016
51. Vanderboor CM, Thibeault PE, Nixon KC, Gros R, Kramer JM, Ramachandran R. Proteinase-Activated Receptor 4 (PAR4) Activation Triggers Cell Membrane Blebbing through RhoA and beta-arrestin. *Mol Pharmacol*. 2020. doi: 10.1124/mol.119.118232
52. Rezaie AR. Protease-activated receptor signalling by coagulation proteases in endothelial cells. *Thromb Haemost*. 2014;112:876-882. doi: 10.1160/th14-02-0167

HIGHLIGHTS

- PAR4 is a low-expressing but highly potent receptor on hepatic endothelial cells *in vivo*.
- PAR1 and PAR4 can act synergistically on hepatic endothelial cells but also possess distinct functions following APAP overdose.
- Alterations in hepatic vascular stability do not contribute to hepatocyte dysfunction after APAP overdose.
- The utilization of translating ribosome affinity purification (TRAP) combined with conditional genetic knockouts for GPCRs represents an innovative *in vivo* method for studying receptor-mediated transcriptional reprogramming following a pathological insult like APAP overdose.

Figure Legends

Figure 1. Deletion of endothelial *Par1* and/or *Par4* reduces APAP-induced permeability in mice. (**A**) Outline of experimental procedures performed on mice. DOB: date of birth; EOD: every other day. (**B**) Schematic of Evans blue dye assay for liver permeability. (**C**) Quantification of Evans blue dye extravasated from livers in saline-treated control mice (black dotted line) and APAP-treated control, *Par1*^{iECko}, *Par4*^{iECko}, and *Par1/4*^{iECko} mice. Data were analyzed by the mixed effects model, and a two-stage linear step-up procedure of Benjamini, Krieger, and Yekutieli was used for multiple comparisons testing. q-values and animal numbers (n) are displayed in the graphs.

Figure 2. Deletion of endothelial *Par1* and/or *Par4* reduces APAP-induced sinusoidal congestion in mice. (Left) Representative images of H&E staining and masking [to reveal red blood cells (RBCs) in black] in APAP-treated livers from littermate control (CON) versus (**A**) *Par1/4*^{iECko}, (**B**) *Par1*^{iECko}, (**C**) *Par4*^{iECko}, and (**D**) *Par4*^{PLTko} mice at 24 hours following overdose. (Right) Quantification of RBC congested areas from histological sections, including in saline (SAL)-treated animals. Data were analyzed by 2-way ANOVA with Tukey's post hoc test (n=3-9 mice/group). Scale bar = 500 μM.

Figure 3. Deletion of endothelial *Par1* and/or *Par4* does not affect APAP-induced hepatocyte necrosis and dysfunction. (**A-D**, Left) Representative images of H&E staining in APAP-treated livers from littermate control (CON) versus (**A**) *Par1/4*^{iECko}, (**B**) *Par1*^{iECko}, (**C**) *Par4*^{iECko}, and (**D**) *Par4*^{PLTko} mice at 6 hours following overdose (scale bar = 500 μM). (**A-D**, Right) Quantification of necrotic lesion area from histological sections, including in saline (SAL)-treated animals. (**E-F**) Serum ALT (**E**) and AST (**F**) levels were measured at 6 and 24 hours after saline (SAL) treatment or APAP overdose in littermate control (CON) and *Par1/4*^{iECko} mice. The reference range is shown with red dotted lines for ALT (28-132 U/L) and AST (59-247 U/L). (**A-D**) Data were analyzed by 2-way ANOVA with Tukey's post hoc test (n=3-9 mice/group); p-values are displayed in the graphs. (**E-F**) Data were analyzed by 3-way ANOVA, and a two-stage linear step-up procedure of Benjamini, Krieger, and Yekutieli was used for multiple comparisons testing (n=3-6 mice/group); q-values are displayed in the graphs.

Figure 4. TRAPseq reveals distinct endothelial and total liver responses to APAP overdose. (A) Outline of TRAPseq protocol; samples were collected at 6 hr after saline or APAP treatment. **(B)** Principal component analysis (PCA) of RNAseq samples. **(C-D)** Volcano plot of APAP-induced gene expression changes in the liver (C) and endothelium (D). **(E)** Venn diagrams of commonly enriched and depleted pathways between the liver and endothelium after APAP overdose.

Figure 5. *Par1* and *Par4* expression analysis within TRAPseq data. (A) *Par1* expression in liver and endothelium of saline-treated $Par1^{ECwt}$, $Par1^{iEChet}$, and $Par1^{iECko}$ mice. **(B)** *Par4* expression in liver and endothelium of saline-treated $Par1^{ECwt}$, $Par4^{iEChet}$, and $Par4^{iECko}$ mice. **(C)** *Par4* expression in liver and endothelium from saline- and APAP-treated mice with heterozygous (het) and homozygous (ko) deletion of endothelial *Par1*. **(D)** *Par1* expression in liver and endothelium from saline- and APAP-treated mice with heterozygous (het) and homozygous (ko) deletion of endothelial *Par4*. Data in A and B were analyzed by 2-way ANOVA with Tukey's post hoc test (n=3); p-values are displayed in the graphs. Data in C and D were analyzed by 3-way ANOVA, and a two-stage linear step-up procedure of Benjamini, Krieger, and Yekutieli was used for multiple comparisons testing (n=3); q-values are displayed in the graphs.

Figure 6. TRAPseq reveals that endothelial PAR1 and PAR4 differentially regulate EC gene expression changes in response to APAP overdose. (A-B) Volcano plots of gene expression changes between control and $Par1^{iECko}$ ECs (A) or $Par4^{iECko}$ ECs (B) after APAP overdose. **(C)** IPA pathways that were differentially regulated between ECs from control and $Par1^{iECko}$ mice after APAP overdose. **(D)** Heatmap of select genes differentially expressed in ECs between control and $Par1^{iECko}$ mice after saline treatment or APAP overdose.

Figure 1

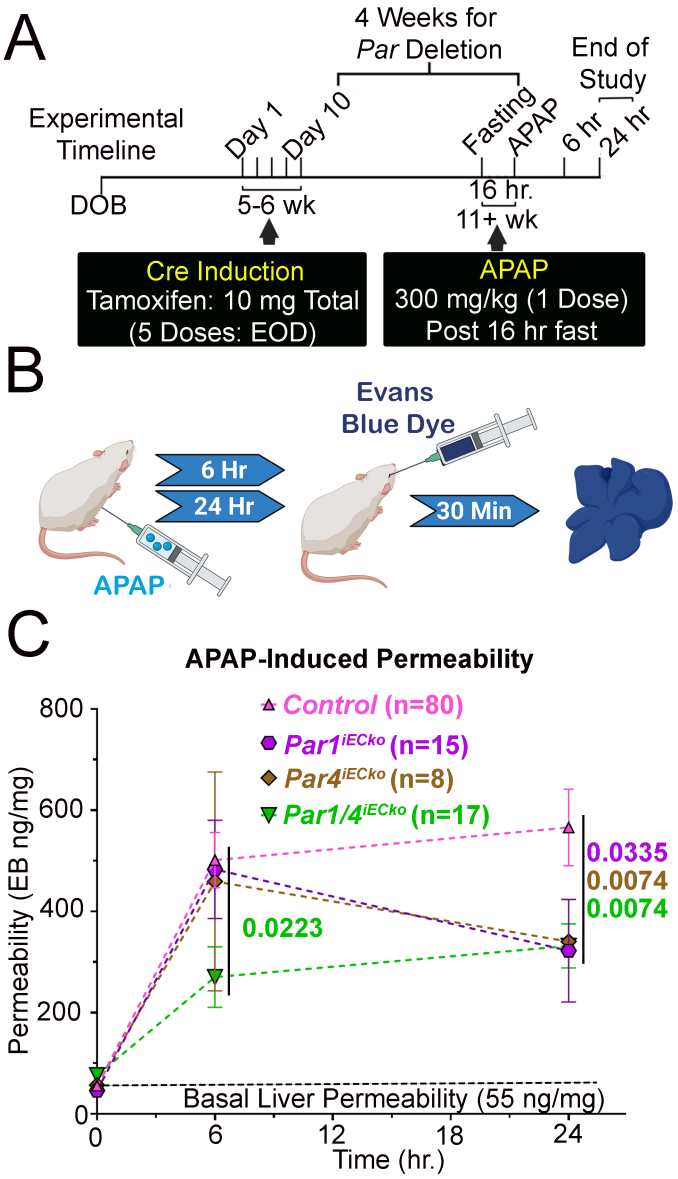
A
4 Weeks for
Par Deletion
End of
Study
Experimental
Timeline
Day 1
Day 10
Fasting
APAP
6 hr
24 hr
DOB
5-6 wk
16 hr.
11+ wk
Cre Induction
Tamoxifen: 10 mg Total
(5 Doses: EOD)
APAP
300 mg/kg (1 Dose)
Post 16 hr fast
B
Evans
Blue Dye
6 Hr
24 Hr
30 Min
APAP
C
APAP-Induced Permeability
Control (n=80)
Par1iECko (n=15)
Par4iECko (n=8)
Par1/4iECko (n=17)
0.0335
0.0074
0.0074
0.0223
Permeability (EB ng/mg)
800
600
400
200
0
Basal Liver Permeability (55 ng/mg)
0
6
12
18
24
Time (hr.)

Figure 2

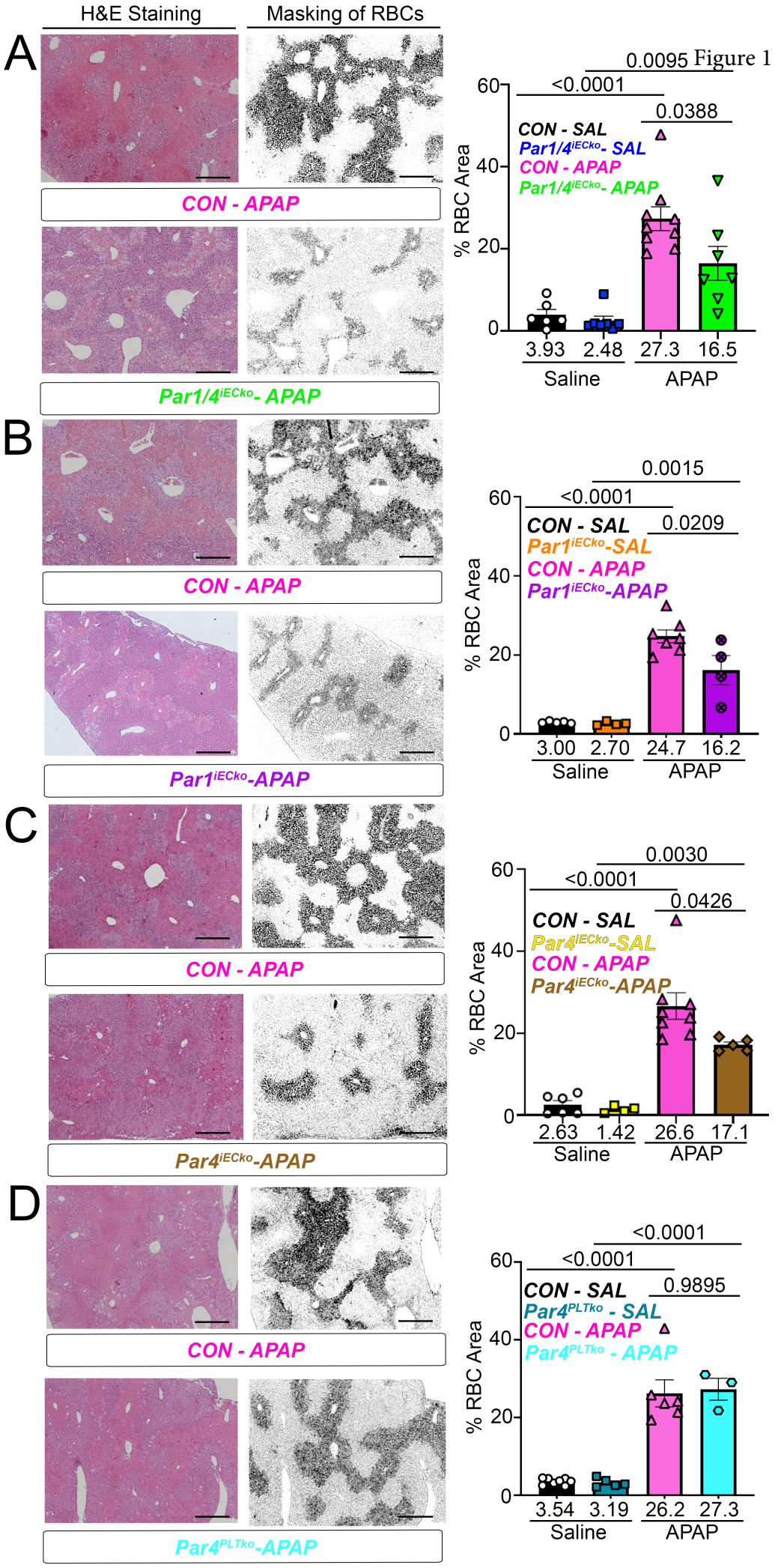
H&E Staining
Masking of RBCs
A
CON - APAP
Par1/4iECko- APAP
0.0095 Figure 1
<0.0001
0.0388
CON - SAL
Par1/4iECko- SAL
CON - APAP
Par1/4iECko- APAP
% RBC Area
60
40
20
0
3.93
2.48
27.3
16.5
Saline
APAP
B
CON - APAP
Par1iECko-APAP
0.0015
<0.0001
0.0209
CON - SAL
Par1iECko-SAL
CON - APAP
Par1iECko-APAP
% RBC Area
60
40
20
0
3.00
2.70
24.7
16.2
Saline
APAP
C
CON - APAP
Par4iECko-APAP
0.0030
<0.0001
0.0426
CON - SAL
Par4iECko-SAL
CON - APAP
Par4iECko-APAP
% RBC Area
60
40
20
0
2.63
1.42
26.6
17.1
Saline
APAP
D
CON - APAP
Par4PLTko-APAP
<0.0001
<0.0001
0.9895
CON - SAL
Par4PLTko - SAL
CON - APAP
Par4PLTko - APAP
% RBC Area
60
40
20
0
3.54
3.19
26.2
27.3
Saline
APAP

Figure 3

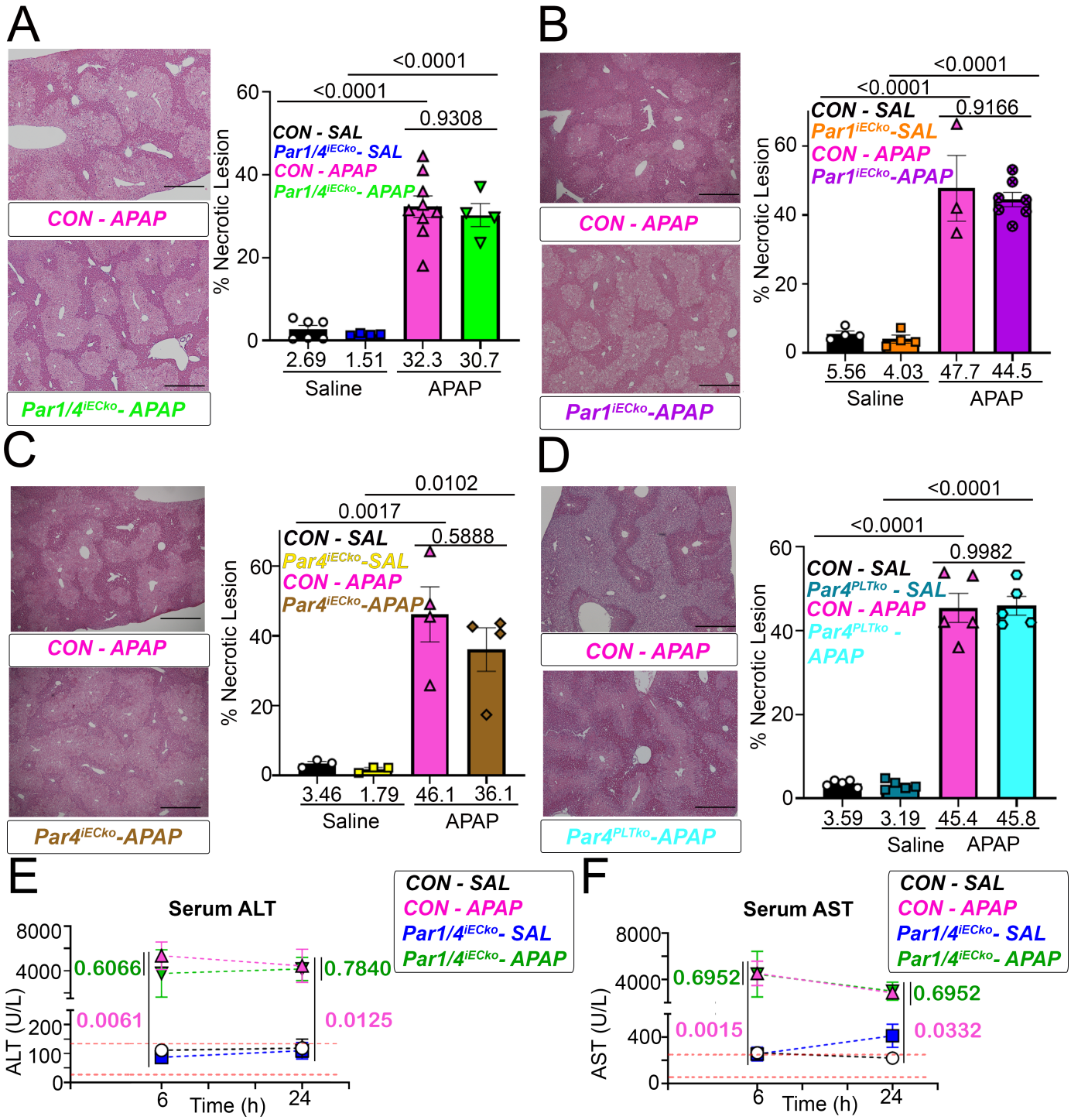
A
CON - APAP
Par1/4iECko- APAP
% Necrotic Lesion
CON - SAL
Par1/4iECko- SAL
CON - APAP
Par1/4iECko- APAP
<0.0001
<0.0001
0.9308
2.69
1.51
32.3
30.7
Saline
APAP
B
CON - APAP
Par1iECko-APAP
% Necrotic Lesion
CON - SAL
Par1iECko-SAL
CON - APAP
Par1iECko-APAP
<0.0001
<0.0001
0.9166
5.56
4.03
47.7
44.5
Saline
APAP
C
CON - APAP
Par4iECko-APAP
% Necrotic Lesion
CON - SAL
Par4iECko-SAL
CON - APAP
Par4iECko-APAP
0.0102
0.0017
0.5888
3.46
1.79
46.1
36.1
Saline
APAP
D
CON - APAP
Par4PLTko-APAP
% Necrotic Lesion
CON - SAL
Par4PLTko - SAL
CON - APAP
Par4PLTko - APAP
<0.0001
<0.0001
0.9982
3.59
3.19
45.4
45.8
Saline
APAP
E
Serum ALT
ALT (U/L)
Time (h)
CON - SAL
CON - APAP
Par1/4iECko- SAL
Par1/4iECko- APAP
0.6066
0.7840
0.0061
0.0125
F
Serum AST
AST (U/L)
Time (h)
CON - SAL
CON - APAP
Par1/4iECko- SAL
Par1/4iECko- APAP
0.6952
0.6952
0.0015
0.0332

Figure 4

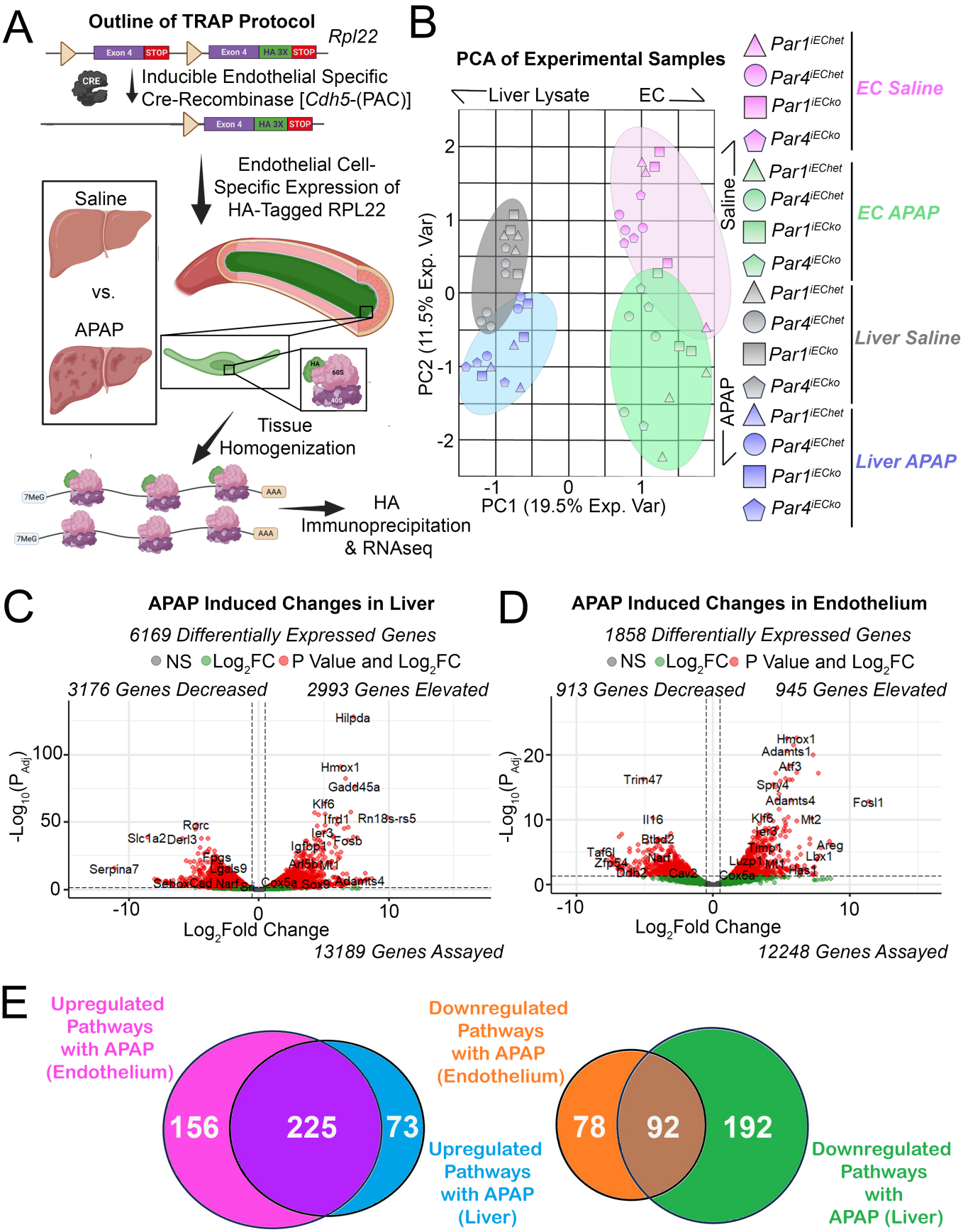

A
Outline of TRAP Protocol
Rpl22
Exon 4
STOP
HA 3X
CRE
Inducible Endothelial Specific Cre-Recombinase [Cdh5-(PAC)]
Endothelial Cell-Specific Expression of HA-Tagged RPL22
Saline
vs.
APAP
HA
60S
40S
Tissue Homogenization
7MeG
AAA
HA Immunoprecipitation & RNAseq
B
PCA of Experimental Samples
Liver Lysate
EC
Saline
APAP
PC2 (11.5% Exp. Var)
PC1 (19.5% Exp. Var)
Par1iEChet
Par4iEChet
Par1iECko
Par4iECko
EC Saline
EC APAP
Liver Saline
Liver APAP
C
APAP Induced Changes in Liver
6169 Differentially Expressed Genes
NS
Log2FC
P Value and Log2FC
3176 Genes Decreased
2993 Genes Elevated
-Log10(PAdj)
Log2Fold Change
13189 Genes Assayed
Hilpda
Hmox1
Gadd45a
Klf6
Ifrd1
Rn18s-rs5
Ier3
Fosb
Igfbp1
Arl5b
Mt1
Adamts4
Rorc
Slc1a2
Derl3
Fpgs
Lgals9
Serpina7
Cox5a
Sox9
D
APAP Induced Changes in Endothelium
1858 Differentially Expressed Genes
913 Genes Decreased
945 Genes Elevated
12248 Genes Assayed
Trim47
Il16
Btbd2
Taf6l
Zfp54
Ddb2
Narf
Cav2
Cox5a
Luzp1
Timp1
Mt1
Has1
Lbx1
Areg
Mt2
Fosl1
Spry4
Atf3
Adamts1
E
Upregulated Pathways with APAP (Endothelium)
156
225
73
Upregulated Pathways with APAP (Liver)
Downregulated Pathways with APAP (Endothelium)
78
92
192
Downregulated Pathways with APAP (Liver)

Figure 5

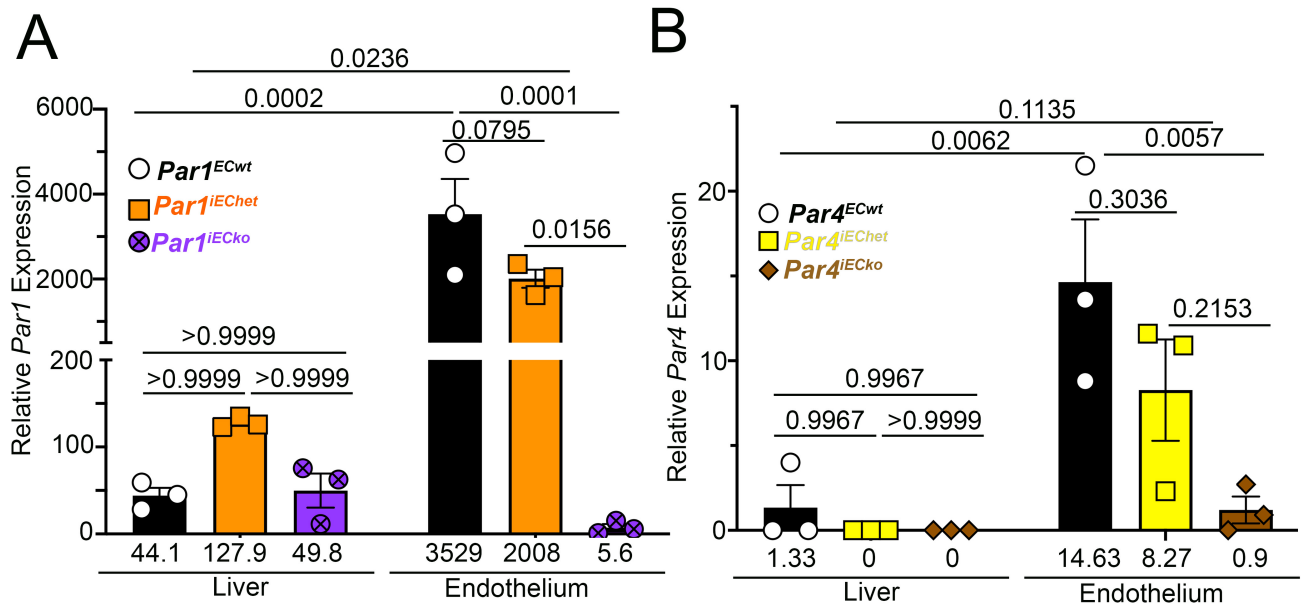
A
0.0236
0.0002
0.0001
0.0795
0.0156
>0.9999
>0.9999
>0.9999
Relative Par1 Expression
Par1ECwt
Par1iEChet
Par1iECko
44.1
127.9
49.8
3529
2008
5.6
Liver
Endothelium
B
0.1135
0.0062
0.0057
0.3036
0.2153
0.9967
0.9967
>0.9999
Relative Par4 Expression
Par4ECwt
Par4iEChet
Par4iECko
1.33
0
0
14.63
8.27
0.9
Liver
Endothelium

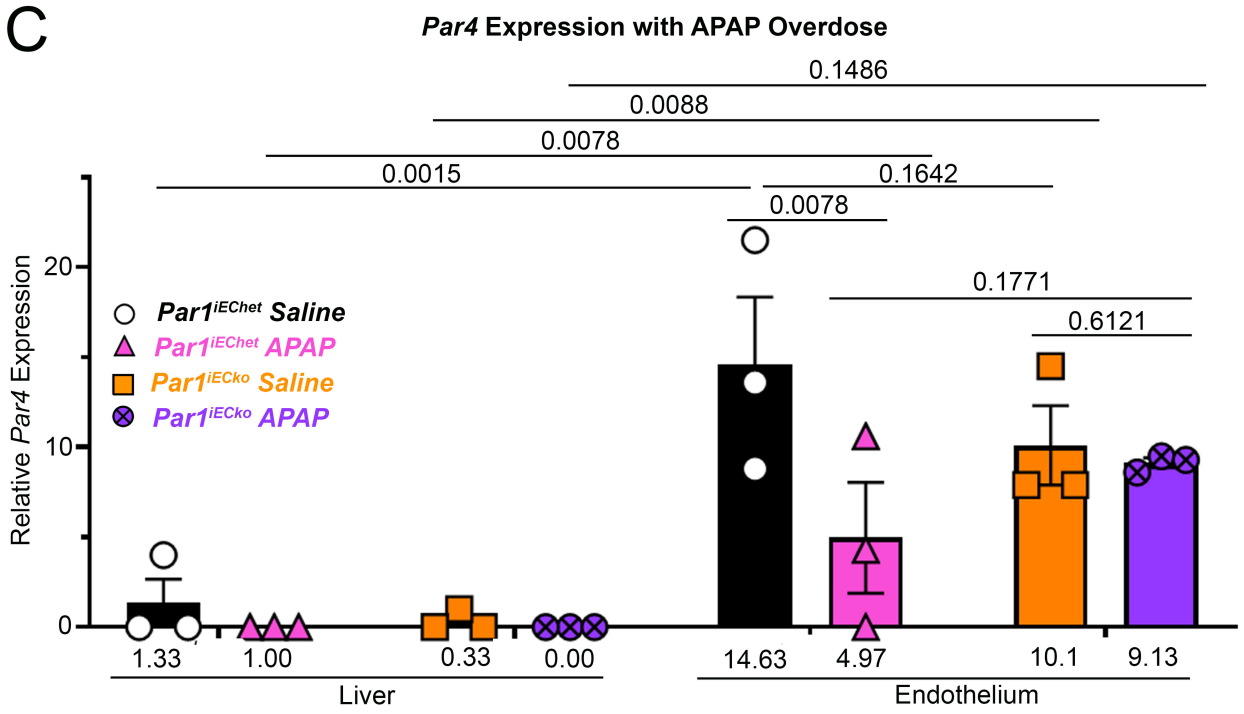
C
Par4 Expression with APAP Overdose
0.1486
0.0088
0.0078
0.0015
0.1642
0.0078
0.1771
0.6121
Relative Par4 Expression
Par1iEChet Saline
Par1iEChet APAP
Par1iECko Saline
Par1iECko APAP
1.33
1.00
0.33
0.00
14.63
4.97
10.1
9.13
Liver
Endothelium

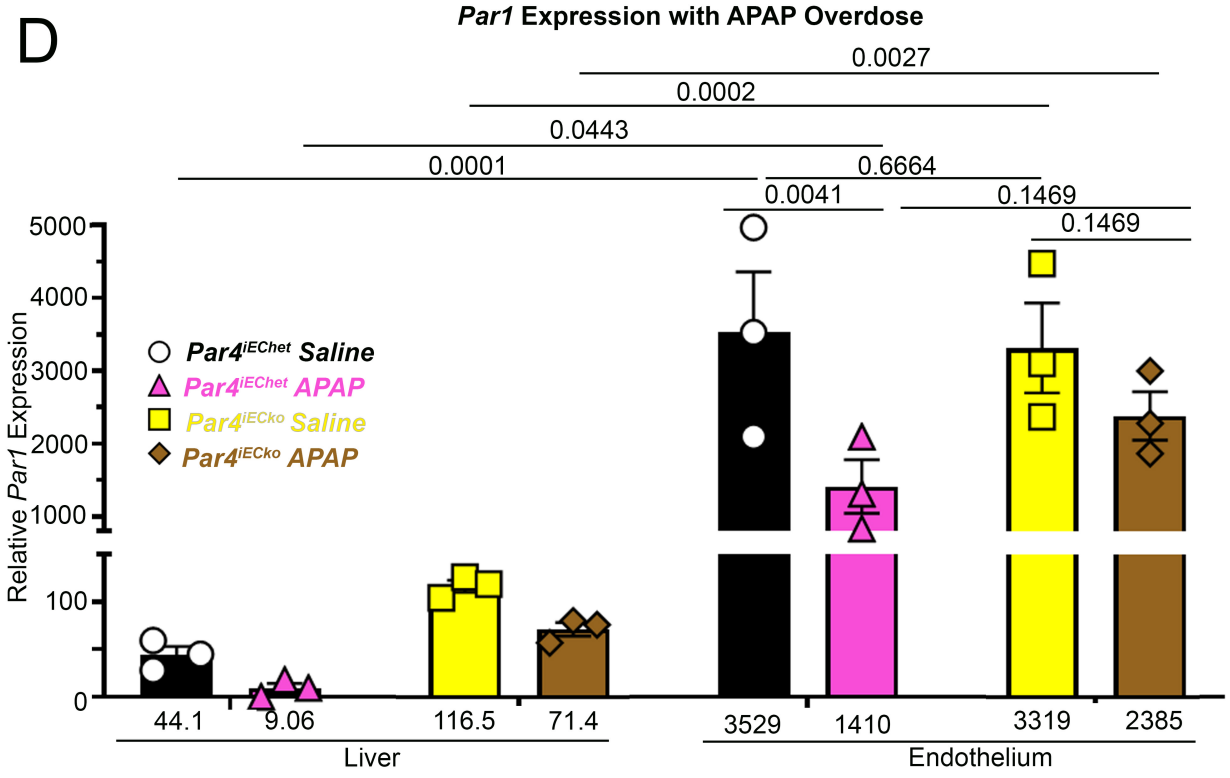
D
Par1 Expression with APAP Overdose
0.0027
0.0002
0.0443
0.0001
0.6664
0.0041
0.1469
0.1469
Relative Par1 Expression
Par4iEChet Saline
Par4iEChet APAP
Par4iECko Saline
Par4iECko APAP
44.1
9.06
116.5
71.4
3529
1410
3319
2385
Liver
Endothelium

Figure 6

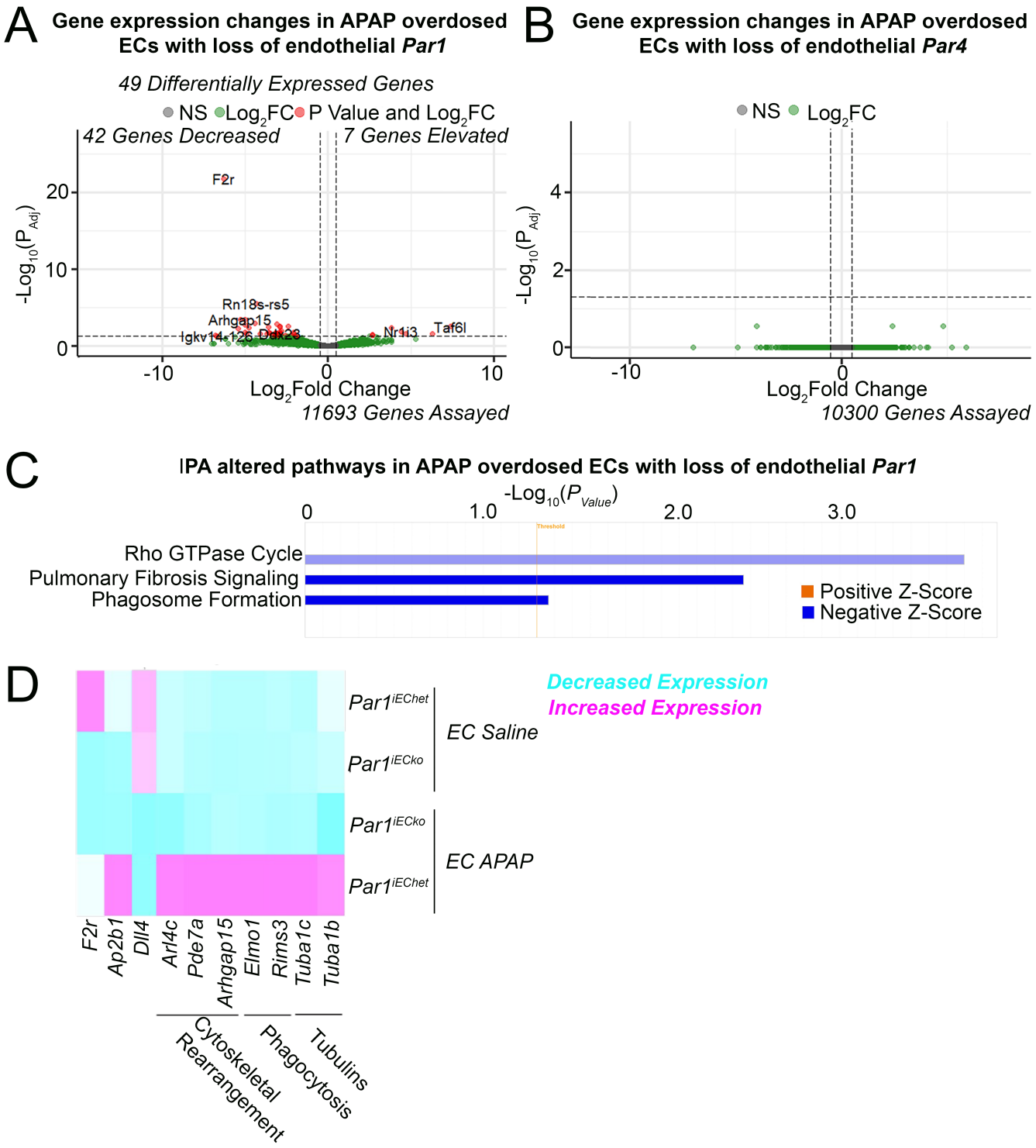
A
Gene expression changes in APAP overdosed ECs with loss of endothelial Par1
49 Differentially Expressed Genes
NS
Log2FC
P Value and Log2FC
42 Genes Decreased
7 Genes Elevated
F2r
Rn18s-rs5
Arhgap15
Igkv14-126
Ddx23
Nr4i3
Taf6l
-Log10(PAdj)
Log2Fold Change
11693 Genes Assayed
B
Gene expression changes in APAP overdosed ECs with loss of endothelial Par4
NS
Log2FC
-Log10(PAdj)
Log2Fold Change
10300 Genes Assayed
C
IPA altered pathways in APAP overdosed ECs with loss of endothelial Par1
-Log10(PValue)
Threshold
Rho GTPase Cycle
Pulmonary Fibrosis Signaling
Phagosome Formation
Positive Z-Score
Negative Z-Score
D
Decreased Expression
Increased Expression
Par1iEChet
Par1iECko
EC Saline
EC APAP
F2r
Ap2b1
Dll4
Arl4c
Pde7a
Arhgap15
Elmo1
Rims3
Tuba1c
Tuba1b
Cytoskeletal Rearrangement
Phagocytosis
Tubulins